

Propagation of acoustic waves in a von-Kármán vortex street like configuration of disclinations

Sébastien Fumeron, Bertrand Berche

Statistical Physics Group, IJL, UMR Université de Lorraine - CNRS 7198 BP 70239, 54506 Vandœuvre les Nancy, France

Fernando Moraes

Departamento de Física, CCEN, Universidade Federal da Paraíba, Caixa Postal 5008, 58051-900, João Pessoa, PB, Brazil

Fernando Santos ‡

Wolfson Centre for Mathematical Biology, Mathematical Institute, University of Oxford, OX1 3LB Oxford, U.K.

Erms Pereira

Escola Politécnica de Pernambuco, Universidade de Pernambuco, Rua Benfíca, 455, Madalena, 50720-001 Recife, PE, Brazil

Abstract. We show that a simple model of 1D array of topological defects in a crystalline environment is able to guide acoustic waves, depending on the angle of the incident wave. We comment on a recently proposed geophysical mechanism explaining the mantle dynamics by the presence, in some crystalline materials there, of wedge disclinations.

PACS numbers: 43.35.+d Ultrasonics, quantum acoustics, and physical effects of sound - 91.60.Lj Acoustic properties - 91.30.Ab Theory and modeling, computational seismology - 91.10.Kg Crystal movements and deformation

Submitted to: *J. Phys.: Condens. Matter*

1. Introduction

Wave propagation in elastic media is of prime interest in a great number of problems in geophysics, ranging from seismology [1, 2] to mineral physics [3, 4, 5]. For example, the microstructural characterization of rocks can efficiently be done from ultrasonic sounding: early works show that measurements of wave speed or attenuation [6, 7], as well as speckle fields [8], carry precious informations to retrieve the inner structure of polycrystalline media where scattering effects prevail. The Earth's crust consists in a set a rigid pieces, the plates, which are moved by the deformations of an underlying layer, the mantle. These plates rub against each other, causing disturbances (such as earthquakes) that radiate seismic energy in the lithosphere. During their propagation, high-frequency primary seismic waves are scattered by randomly distributed heterogeneties, such as faults, irregular topography of inner layers or space variations of rocks properties. As a result of scattering events, the energy carried by ultrasonic waves is known to obey the radiative transfer equation (RTE), that is a Boltzmann equation that corresponds to a local balance on a radiometric quantity, the specific intensity [9, 10].

In this geophysics context, the mantle dynamics and its ability to deform was recently explained by the presence of wedge disclinations inside olivine-rich rocks [11, 12]. This addresses the challenging problem of ultrasound wave propagation and energy concentration in the presence of topological defects, which is the object of this article. The structure of a wedge disclination can be easily understood from a Volterra "cut-and-glue" process: 1) a cut is made in an elastic cylinder, 2) a wedge of material is removed (positive Frank angle) or added (negative Frank angle) and 3) the two edges of the cut are glued together. Fig.1 shows the Volterra process for the creation of a positive disclination in an elastic disc. If the disc is allowed to buckle into the third dimension, it becomes a cone which shares geometric properties with the disclinated disc: they are both described by an otherwise flat metric with a curvature singularity at the origin. Obviously, for real three-dimensional materials, stress builds up since buckling is not allowed because it would have to be into the fourth space dimension. Single disclinations are then energetically unfavorable in 3D solid crystals because of their too high elastic cost.

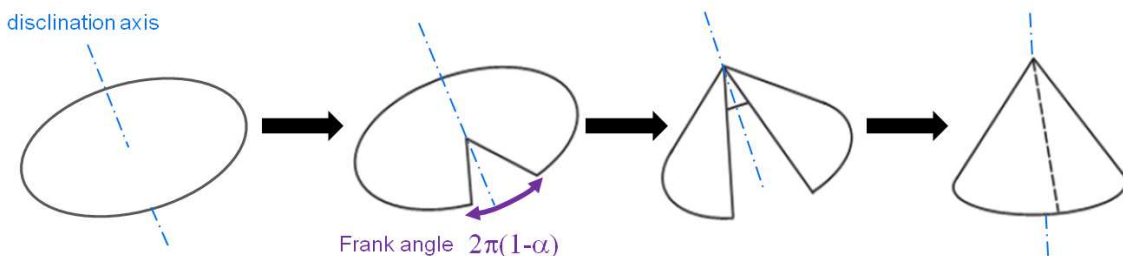


Figure 1. Volterra cut-and-glue process for a disclination.

However, that energy cost can be reduced in specific self-screening configurations involving wedge disclinations dipoles: as considered in [11], the self-screening reveals to be very efficient for olivine presenting a periodic wedge disclination array of alternate Frank angle signs.

In this work, we study the transport of scalar bulk waves in the presence of an array of disclination dipoles. In the first part, we build a geometric model for the distribution of disclinations that was considered in [11], and the main properties of geodesic paths followed by the waves are discussed. Then, we examine the foundations of the radiative transfer equation for the specific intensity from the standpoint of kinetic theory. Finally, the complete form of the non-stationary RTE in the presence of the defects is presented and analyzed, allowing for a discussion of focusing/defocusing of the energy in the system.

2. The von Kármán vortex street geometry

General relativity is the standard example where a physical phenomenon (gravity) is represented by geometrical properties (curvature, torsion). As testified by analogue gravity models [13, 14], the relevance of differential geometry does not restrict to gravitation, but it can also be used for a wide range of classical and quantum systems electromagnetic waves [15, 16], superfluid helium [17], 2D electrons gas [18, 19], liquid crystals [20]...). The pioneering works of Katanaev and Volovich [21] showed the efficiency of this geometric approach to investigate the propagation of elastic waves in the presence of topological defects such as screw dislocations, edge dislocations or disclinations. Single disclinations are line sources of curvature and they correspond to the generation of a conical geometry, as shown in Fig. 1.

In this section, we describe an array of disclination dipoles in terms of differential geometry. Consider two rows made of an infinite number of alternate disclinations separated by distance $2a$ and the rows by $2b$. As illustrated in Fig.2, the positive disclinations (red contours) are at points $(na, (-1)^nb), n \in \mathbb{Z}$, while negative disclinations (blue contours) have coordinates $(na, (-1)^{(n+1)}b), n \in \mathbb{Z}$. Then, following

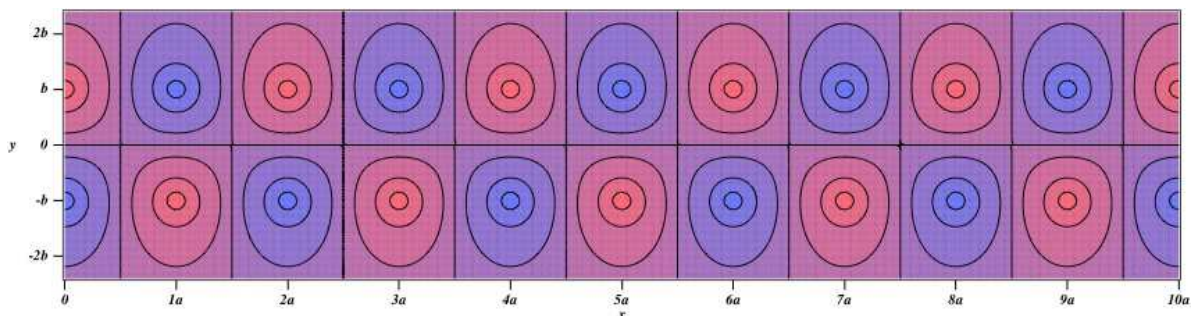


Figure 2. A representation of the von Kármán vortex street distribution of alternate disclinations given by the contour plot of the "potential" (14).

a procedure given in [22], the corresponding background geometry is generally described

by the spacetime line element

$$ds^2 = -c^2 dt^2 + e^{-4V(x,y)} (dx^2 + dy^2) + dz^2 = g_{\mu\nu} dx^\mu dx^\nu. \quad (1)$$

c would be the velocity of light in the general relativity context, but here it stands for the local speed of wave packet, $g_{\mu\nu}$ is the metric tensor (Greek indices run from 0 (time index) to 3 and the Einstein summation convention on repeated indices is used [23]). In the function

$$V(x, y) = (1 - \alpha)f_V(x, y), \quad (2)$$

α is related to the topological charge of a single disclination, whereas f_V describes the space distribution of the defects. Such distribution of defects gives rise to a non-zero curvature tensor component [22]:

$$R_{xyxy} = 2(1 - \alpha)e^{4(1-\alpha)f_V} (\partial_{xx} + \partial_{yy})f_V. \quad (3)$$

In the case of a single row of alternate defects at $y = b$ (positive disclinations at $\dots - 4a, -2a, 0, 2a, 4a\dots$ and negative disclinations at $\dots - 3a, -a, a, 3a\dots$), this function writes

$$f_V(x, y) = \frac{1}{2} \sum_{p=-\infty}^{+\infty} \{ \ln [(x - 2pa)^2 + (y - b)^2] - \ln [(x - [2p - 1]a)^2 + (y - b)^2] \} \quad (4)$$

$$= \frac{1}{2} \sum_{n=-\infty}^{+\infty} (-1)^n \ln [(x - na)^2 + (y - b)^2] \quad (5)$$

and the curvature becomes

$$(\partial_{xx} + \partial_{yy})f_V \propto \sum_{p=-\infty}^{+\infty} [\delta(x - 2pa) - \delta(x - (2p - 1)a)] \delta(y - b). \quad (6)$$

Introducing the complex variable $\xi = x + i(y - b)$, one obtains

$$2f_V(x, y) = \sum_{n=-\infty}^{+\infty} (-1)^n \ln [(\xi - na)(\bar{\xi} - na)] \quad (7)$$

$$= \ln(\xi\bar{\xi}) + \sum_{n=1}^{+\infty} (-1)^n \ln [(\xi^2 - n^2 a^2)(\bar{\xi}^2 - n^2 a^2)] \quad (8)$$

$$= 2\hat{f}_V + 4 \sum_{n=1}^{+\infty} \ln(an), \quad (9)$$

where $\bar{\xi}$ denotes the complex conjugate and the function \hat{f}_V can be obtained by separating odd and even contributions in (5)

$$2\hat{f}_V(\xi) = \ln \left[\xi \prod_{m=1}^{+\infty} \left(1 - \frac{\xi^2}{4m^2 a^2} \right) \bar{\xi} \prod_{p=1}^{+\infty} \left(1 - \frac{\bar{\xi}^2}{4p^2 a^2} \right) \right] \\ - \ln \left[\prod_{m=1}^{+\infty} \left(1 - \frac{\xi^2}{(2m-1)^2 a^2} \right) \prod_{p=1}^{+\infty} \left(1 - \frac{\bar{\xi}^2}{(2p-1)^2 a^2} \right) \right]. \quad (10)$$

From (6), it appears that the singular structure is left invariant when adding a constant to \hat{f}_V . Therefore (9) and (10) represent the same geometry up to a scaling factor. By using the identities

$$\sin(x) = x \prod_{m=1}^{+\infty} \left[1 - \left(\frac{x}{m\pi} \right)^2 \right], \quad \cos(x) = \prod_{m=1}^{+\infty} \left[1 - \left(\frac{2x}{(2m-1)\pi} \right)^2 \right], \quad (11)$$

it finally comes that

$$\hat{f}_V(x, y) = \ln \left| \sin \left(\frac{\pi}{2a} [x + i(y - b)] \right) \right| - \ln \left| \cos \left(\frac{\pi}{2a} [x + i(y - b)] \right) \right| \quad (12)$$

$$= \frac{1}{2} \ln \left[\frac{\cosh^2 \left(\frac{\pi}{2a} (y - b) \right) - \cos^2 \left(\frac{\pi x}{2a} \right)}{\cosh^2 \left(\frac{\pi}{2a} (y - b) \right) - \sin^2 \left(\frac{\pi x}{2a} \right)} \right]. \quad (13)$$

Therefore, when considering two lines of alternate disclinations as in Fig. 2, the function \hat{f}_V becomes:

$$\hat{f}_V(x, y) = \frac{1}{2} \ln \left[\left(\frac{\cosh^2 \left(\frac{\pi}{2a} (y - b) \right) - \cos^2 \left(\frac{\pi x}{2a} \right)}{\cosh^2 \left(\frac{\pi}{2a} (y - b) \right) - \sin^2 \left(\frac{\pi x}{2a} \right)} \right) \left(\frac{\cosh^2 \left(\frac{\pi}{2a} (y + b) \right) - \sin^2 \left(\frac{\pi x}{2a} \right)}{\cosh^2 \left(\frac{\pi}{2a} (y + b) \right) - \cos^2 \left(\frac{\pi x}{2a} \right)} \right) \right] \quad (14)$$

We can think of this function (in fact $V(x, y)$) as a sort of gravitational "potential" acting on point masses that move in the presence of the arrays of defects (see, for example, reference [24]).

As a consequence, the paths followed by acoustic waves are no longer straight lines, but they are the geodesics of the von Kármán vortex street geometry, that is trajectories of shortest lengths in that geometry. They obey the so-called geodesic equations:

$$\frac{d^2 x^\mu}{d\lambda^2} + \Gamma_{\rho\sigma}^\mu \frac{dx^\rho}{d\lambda} \frac{dx^\sigma}{d\lambda} = 0, \quad (15)$$

where λ is an affine parameter along the path and $\Gamma_{\rho\sigma}^\mu$ are the Christoffel connections which can be expressed from the metric tensor components as

$$\Gamma_{\rho\sigma}^\mu = \frac{g^{\mu\nu}}{2} (\partial_\rho g_{\nu\sigma} + \partial_\sigma g_{\nu\rho} - \partial_\nu g_{\rho\sigma}) \quad (16)$$

since there is no torsion. After some calculations, (15) reduce to [22]:

$$\ddot{x} - 2(\dot{x}^2 - \dot{y}^2) \partial_x V - 4\dot{x}\dot{y} \partial_y V = 0, \quad (17)$$

$$\ddot{y} - 2(\dot{x}^2 - \dot{y}^2) \partial_y V - 4\dot{x}\dot{y} \partial_x V = 0. \quad (18)$$

Although the geodesics' system of differential equations above are analytical by nature, the inherent complexity of $f_V(x, y)$ in Eq. (4) leads us to cumbersome expressions for the system in Eq. (18). We circumvent such complexity by using symbolic algebra, thus yielding a quite complex system of differential equations for the geodesics, as illustrated in a flexible Maple code, available from the authors upon request, for arbitrary α , a , and b . In order to get both quantitative and qualitative informations about the geodesics in the von Kármán street, we systematically solved the system of geodesic equations. We fixed $\alpha = 1/2$, $a = 1$, $b = 0.5$ and solved numerically the resulting system of differential equations. Without loss of generality, we chose geodesics starting at the origin, $(x_0(0) = 0, y_0(0) = 0)$, with unitary initial "speed",

$x'(0) = \cos(\theta_0)$, $y'(0) = \sin(\theta_0)$, which defines the shooting angle. In Fig. 3 we illustrate some geodesics in the von Kármán vortex street for a few shooting angles. In Fig. 4 we depict some geodesics in the potential landscape.

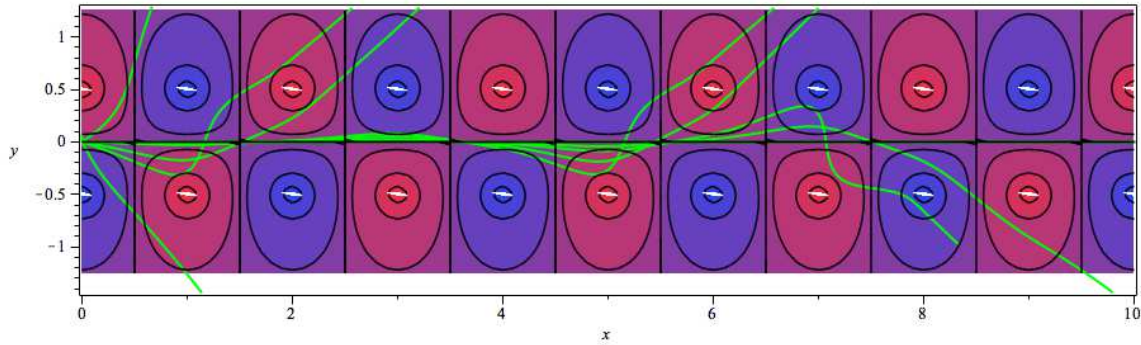


Figure 3. Different geodesics, shot from the origin, in the von Kármán vortex street geometry. Depending on the shooting angle, the propagation of the acoustic wave may be guided by the street of topological defects.

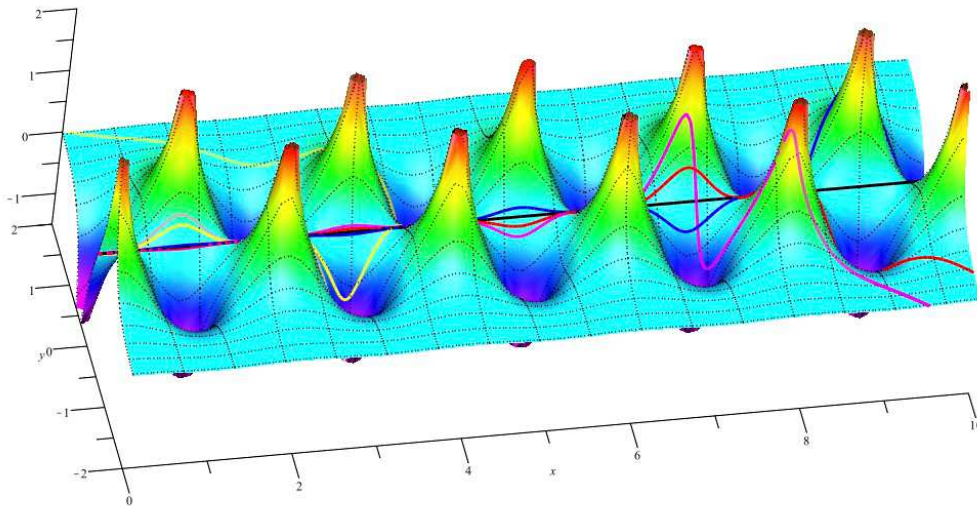


Figure 4. Geodesics in the von Kármán vortex street in the potential landscape.

The acoustic rays, as represented by the geodesics seen in Figs. 3 and 4, are very sensitive to the shooting angle. Furthermore, they appear to be attracted by the positive

defects while repelled by the negative ones. This is quite natural, since the former have the geometry of a cone (with less space than the plane) and the latter of an anticone (with more space than the plane). This makes the geodesic bend toward the positive defect and away from the negative defect. In other words, the rays give a feeling on how acoustic propagation occurs in the medium with an array of defects. We can infer that the defects may be used to design acoustic devices like lenses or waveguides, which previously requires an accurate model to understand how energy is carried along these geodesics. This is the subject of the following section.

3. Radiative transfer equation and Clausius invariant

Originally, radiative transfer consists in a phenomenological description of the interactions of infrared electromagnetic waves with participating matter. Based on the pioneering works by Khvolson [25], Schuster [26] and Schwarzschild [27], this theory borrows concepts from radiometry (measurable quantity such as the radiative flux), classical optics (Fermat principle to get the optical paths) and quantum theory (Planck blackbody function to account for the thermal emission by matter). In this section, we introduce the essential concepts needed for the rest of the paper and we remind the essentials of this phenomenological approach.

The central quantity is the specific intensity I_ν that corresponds to the amount of energy crossing an element dA^2 of area during time dt , in a frequency range between ν and $\nu + d\nu$, and within an element $d\Omega^2$ of unit solid angle centered on direction Ω according to [28] (see Fig. 5):

$$I_\nu = \frac{dE}{\cos \theta dt dA^2 d\nu d\Omega^2}. \quad (19)$$

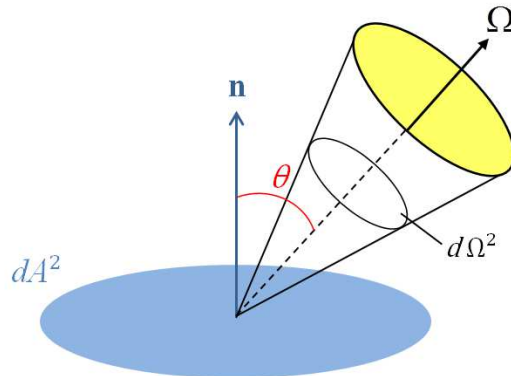


Figure 5. Definition of the specific intensity.

The equation governing I_ν (known as the RTE) is derived from a simple energy balance along any energy path: specific intensity decays ought to absorption and scattering processes, and it gets stronger because of scattering and inner source terms.

In its usual form, it is therefore given by [28, 29]:

$$\frac{d}{ds} I_\nu(t, \mathbf{r}, \boldsymbol{\Omega}) = - \left(\frac{1}{l} + \frac{1}{l_a} \right) I_\nu(t, \mathbf{r}, \boldsymbol{\Omega}) + S(t, \mathbf{r}, \boldsymbol{\Omega}), \quad (20)$$

where d/ds is the total path length derivative, l is the scattering mean free path, l_a is the absorption length, where both can depend on the position. The source term writes

$$S(t, \mathbf{r}, \boldsymbol{\Omega}) = \frac{1}{l} \int_{4\pi} p(\boldsymbol{\Omega}', \boldsymbol{\Omega}) I_\nu(t, \mathbf{r}, \boldsymbol{\Omega}') d^2\Omega' + S^0(t, \mathbf{r}, \boldsymbol{\Omega}). \quad (21)$$

Here, $p(\boldsymbol{\Omega}', \boldsymbol{\Omega})$ is the probability that a beam propagating in direction $\boldsymbol{\Omega}$ is scattered in direction $\boldsymbol{\Omega}'$ and S^0 is due to the radiative energy emitted by sources embedded in the medium. This last term will be neglected in the remainder of this work. This equation is relevant for the present context, since it also applies for the acoustic waves (compression, no shear) propagating in elastic media [10, 9].

Despite its handiness, the phenomenological approach hides some intricate points. Indeed, anytime a symmetry of physical properties of the participating medium is lost, (20) must be modified. As a matter of fact, in nonstationnary and graded-index media, the adiabatic invariant along a path is no longer the specific intensity but the so-called Clausius invariant [30]:

$$C_\nu = \frac{I_\nu}{n(\mathbf{r})^2 \nu^3}, \quad (22)$$

where $n(\mathbf{r})$ is the refractive index (the same result was also found from other arguments by [31, 32, 33, 34]). It must be emphasized that (22) also holds for radiative transfer of acoustic waves, as an analog of Fermat principle can be obtained in elastodynamics [35]. Hence, considering the balance on Clausius invariant, the modified RTE now writes as [34]:

$$\frac{d}{ds} C_\nu = - \left(\frac{1}{l} + \frac{1}{l_a} \right) C_\nu + \frac{1}{l} \int_{4\pi} p(\boldsymbol{\Omega}', \boldsymbol{\Omega}) C_\nu d^2\Omega'. \quad (23)$$

Integral solutions of (23) can be deduced formally by the variation of parameters. One illustrates this point considering the simple case of a steady-state regime

$$\begin{aligned} \frac{I_\nu}{n^2}(s, \boldsymbol{\Omega}) &= \frac{I_\nu}{n^2}(s_0, \boldsymbol{\Omega}_0) \exp \left(- \int_{s_0}^s \frac{ds'}{l(s') + l_a(s')} \right) \\ &+ \int_{s_0}^s \tilde{S}(s', \boldsymbol{\Omega}) \exp \left(- \int_{s'}^s \frac{ds''}{l(s'') + l_a(s'')} \right) ds', \end{aligned} \quad (24)$$

with

$$\tilde{S}(t, \mathbf{r}, \boldsymbol{\Omega}) = \frac{1}{l} \int_{4\pi} p(\boldsymbol{\Omega}', \boldsymbol{\Omega}) \frac{I_\nu(t, \mathbf{r}, \boldsymbol{\Omega}')}{n(\mathbf{r})^2} d^2\Omega'. \quad (25)$$

It is important to recall that in (23)-(25), the balance is performed along ray paths. Whether it is electromagnetic or elastic beams [35], the ray paths obey Fermat principle which, as previously stated, requires to determine the refractive index. In the next section, we introduce the distribution of disclination dipoles from a geometric standpoint and extract from it the effective refractive index experienced by the acoustic waves.

4. Radiative transfer equation in the von Kármán vortex street geometry

Based on the two preceding sections, we are now focusing on the modified RTE in the presence of the array of disclinations and determine some of its most remarkable properties. First, we briefly present the general procedure to obtain the effective refractive index from a diagonal metric. Consider a wave propagating along direction $\mathbf{\Omega} = (\sin \hat{\theta} \cos \hat{\phi}, \sin \hat{\theta} \sin \hat{\phi}, \cos \hat{\theta})$ ($\hat{\theta}$ and $\hat{\phi}$ denote the polar and azimuthal angles) in a geometric background described by the metric tensor $g_{\mu\nu}$, then the dispersion relation of a wave associated to 4-wavevector $K^\mu = (\omega/c, k \sin \hat{\theta} \cos \hat{\phi}, k \sin \hat{\theta} \sin \hat{\phi}, k \cos \hat{\theta})$ writes as $K^\mu g_{\mu\nu} K^\nu = 0$, which gives

$$-\frac{\omega^2}{c^2} |g_{00}| + k^2 \left(g_{11} \sin^2 \hat{\theta} \cos^2 \hat{\phi} + g_{22} \sin^2 \hat{\theta} \sin^2 \hat{\phi} + g_{33} \cos^2 \hat{\theta} \right) = 0, \quad (26)$$

(all space components g_{ii} are positive). On the other hand, the dispersion relation of a wave in a dielectric medium at rest and of refractive index n is given by:

$$-\frac{\omega^2}{c^2} n^2 + k^2 = 0. \quad (27)$$

Substituting k^2 from (27) into (26) defines an effective refractive index

$$n(\mathbf{r}, \mathbf{\Omega}) = \sqrt{\frac{|g_{00}|}{g_{11} \sin^2 \hat{\theta} \cos^2 \hat{\phi} + g_{22} \sin^2 \hat{\theta} \sin^2 \hat{\phi} + g_{33} \cos^2 \hat{\theta}}}. \quad (28)$$

Generally speaking, this refractive index depends both on the position in the medium through the radial vector \mathbf{r} and the local propagation direction $\mathbf{\Omega}$, but it does not exhibit any dispersion.

In the case of the von Kármán vortex street, the effective refractive index writes as

$$n(\mathbf{r}, \hat{\theta}) = \frac{1}{\sqrt{e^{-4V(x,y)} \sin^2 \hat{\theta} + \cos^2 \hat{\theta}}}. \quad (29)$$

Notice that the refractive index depends both on the position (x, y) and on the local propagation direction $\hat{\theta}$. In Fig. 6 it is presented a plot of $n(\mathbf{r}, \hat{\theta})$ along selected geodesics, showing strong fluctuations in the vicinity of the defects.

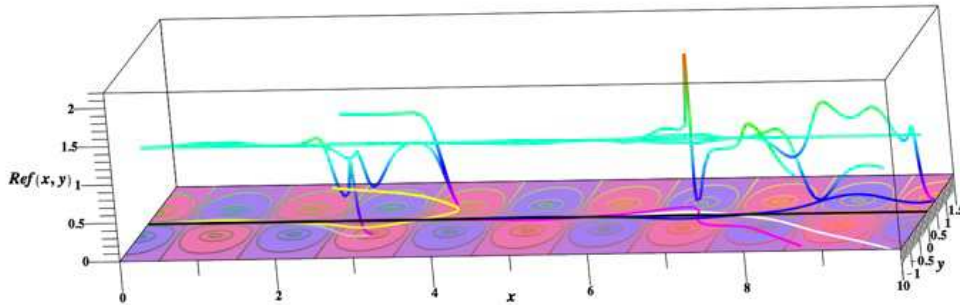


Figure 6. Refraction index projected on the von Kármán vortex street along some representative geodesics. The refraction index is nearly constant far from the defects and fluctuates around them.

While the metric exhibits translational symmetry along the z axis, hence the coefficients $g_{\mu\nu}$ do not depend on z , this is not true for the effective refractive index which looses this symmetry through the dependence on the wavevector direction. From this perspective, Eq.(29) might be misleading since only the angle $\hat{\theta}$ appears explicitly, but the presence of the azimuthal angle $\hat{\phi}$ is implicit in the x, y dependence. From (22), one deduces the corresponding Clausius invariant

$$C_\nu(t, \mathbf{r}, \boldsymbol{\Omega}) = \frac{I_\nu(t, \mathbf{r}, \boldsymbol{\Omega})}{\nu^3} \left(e^{-4V(x,y)} \sin^2 \hat{\theta} + \cos^2 \hat{\theta} \right). \quad (30)$$

Therefore, the modified RTE (MRTE) in the presence of the array of defects is given by

$$\begin{aligned} \frac{d}{ds} \left[\frac{I_\nu(t, \mathbf{r}, \boldsymbol{\Omega})}{\nu^3} \left(e^{-4V(x,y)} \sin^2 \hat{\theta} + \cos^2 \hat{\theta} \right) \right] &= - \left(\frac{1}{l} + \frac{1}{l_a} \right) \frac{I_\nu(t, \mathbf{r}, \boldsymbol{\Omega})}{\nu^3} \left(e^{-4V(x,y)} \sin^2 \hat{\theta} + \cos^2 \hat{\theta} \right) \\ &+ \frac{1}{l} \int_{4\pi} p(\boldsymbol{\Omega}, \boldsymbol{\Omega}') \frac{I_\nu(t, \mathbf{r}, \hat{\mathbf{s}}')}{\nu^3} \left(e^{-4V(x,y)} \sin^2 \hat{\theta} + \cos^2 \hat{\theta} \right) d^2 \hat{\mathbf{s}}' + S(t, \mathbf{r}, \boldsymbol{\Omega}). \end{aligned} \quad (31)$$

Some physical insights can be obtained by comparing Eq. (31) to the one without defects (20). First, let us consider the simple steady-state case in a non-participating medium which writes phenomenologically as

$$\frac{dI_\nu}{ds} = \left(2 \frac{d}{ds} \ln n \right) I_\nu = - \frac{I_\nu}{l_\alpha}. \quad (32)$$

Following [30], this defines a typical length which measures the spatial inhomogeneities, l_α , given by

$$\begin{aligned} \frac{1}{l_\alpha(x, y, \hat{\theta})} &= \frac{2 \sin \hat{\theta}}{(e^{-4V(x,y)} - 1) \sin^2 \hat{\theta} + 1} \left[2 \sin \hat{\theta} e^{-4V(x,y)} \left(\frac{\partial V}{\partial x} \frac{dx}{ds} + \frac{\partial V}{\partial y} \frac{dy}{ds} \right) \right. \\ &\quad \left. + \cos \hat{\theta} (e^{-4V(x,y)} - 1) \frac{d\hat{\theta}}{ds} \right]. \end{aligned} \quad (33)$$

The first derivatives dx/ds , dy/ds and $d\hat{\theta}/ds$ are obtained numerically from the geodesic equations (15). There is no constraint that settles the signs of the different terms involved in l_α : hence, this parameter can be either of positive or of negative sign, so that the array of defects either damps or amplifies locally the specific intensity. That means that the von Kármán vortex street does not only curve the geodesics, but it also leads to a local geometric reduction/enhancement of energy carried by the waves. Although (32) is analog to a Beer-Lambert law, it must be emphasized that there is no absorption process here. The *inhomogeneity length* (33) rather describes the local spatial enhancement (where it is negative) or local spatial reduction (where it is positive) of the acoustic wave, like a focusing/defocusing effect. Curvature doping of radiant intensity is well-known in radiative transfer and was first discussed in [15]. This might be at the origin of the deformation of the medium, where the energy transported by the acoustic waves is locally amplified, allowing for a physical mechanism for the mantle deformation due to the presence of topological defects, as proposed in [11].

5. Concluding remarks

To sum up, we proposed a simple toy-model for acoustic waves propagation through a distribution of disclinations inside olivine-rich rocks. In the presence of two rows of alternate wedge disclinations, two new phenomena arise. First, sound paths are curved by an effective background geometry, presenting alternate regions of positive and negative curvature originating from the alternate disclinations themselves. Second, as testified by the change in Clausius invariant, the energy carried by beams can be geometrically amplified/attenuated depending on the direction of the propagation. These two effects seem extremely sensitive to shooting conditions.

Moreover, an asset of this formalism is that although polarization states of the waves and mode coupling effects were not explicitly discussed, they can formally be incorporated from the above results to obtain the generalization of the elastic transfer equation. Investigating their impact on transfer will be the object of our further investigations.

- [1] H. Sato, M. Fehler, *Seismic Wave Propagation and Scattering in the Heterogeneous Earth*. AIP Press/Springer-Verlag, New York, pp. 1-308 (1998).
- [2] A. Kaufman, A.L. Levshin, *Acoustic and Elastic Wave Fields in Geophysics, Part I, Volume 37 in Methods in Geochemistry and Geophysics* (2000).
- [3] K. Goebbels, Ultrasonics for microcrystalline structure examination, *Phil. Trans. R. Soc. London Set. A* **320**, 161-169 (1986).
- [4] J.A. Turner and R.L. Weaver, Radiative transfer and multiple scattering of diffuse ultrasound in polycrystalline media. *The Journal of the Acoustical Society of America*, 96(6), 3675-3683 (1994).
- [5] P. Anugonda, J.S. Wiehn and J.A. Turner, Diffusion of ultrasound in concrete. *Ultrasonics*, **39**(6), 429-435 (2001).
- [6] W.P. Mason and H.J. McSkimm, Attenuation and scattering of high frequency sound waves in metals and glasses, *J. Acoust. Soc. Am.* **19**, 464-473 (1947).
- [7] A. Vary, Ultrasonic measurement of material properties, in *Research Techniques in Nondestructive Testing V. IV*, edited by R. S. Sharpe (Academic, New York, 1980).
- [8] K. Goebbels, Structure analysis by scattered ultrasonic radiation, in *Research Techniques in Nondestructive Testing V. IV*, edited by R. S. Sharpe (Academic, New York, 1980).
- [9] L. Margerin, Introduction to radiative transfer of seismic waves. *GEOPHYSICAL MONOGRAPH-AMERICAN GEOPHYSICAL UNION*, **157**, p. 229 (2005).
- [10] J.A. Turner and R.L. Weaver. Radiative transfer of ultrasound. *The Journal of the Acoustical Society of America*, **96**(6), 3654-3674 (1994).
- [11] P. Cordier, S. Demouchy, B. Beausir, V. Taupin, F. Barou and C. Fressengeas, Disclination provide the missing mechanism for deforming olivine-rich rocks in the mantle, *Nature* **507** (2014).
- [12] G. Hirth, Earth science: missing link in mantle dynamics, *Nature* **507**, 42-43 (06 March 2014).
- [13] F. Moraes, Condensed matter physics as a laboratory for gravitation and cosmology, *Braz. J. Phys.* **30** (2) São Paulo (2000).
- [14] C. Barcelo, S. Liberati and M. Visser, Analogue gravity, *Living Rev. Relativity* **8** 12 (2005).
- [15] P. Ben-Abdallah, When the space curvature dopes the radiant intensity, *JOSA B* **19** (8) (2002), pp. 1766-1772.
- [16] S. Fumeron, B. Berche, F. Santos, E. Pereira, and F. Moraes, Optics near a hyperbolic defect, *Phys. Rev. A* **92**, 063806 (2015).
- [17] G.E. Volovik, *The Universe in a Helium Droplet*, vol. 117 of International Series of Monographs on Physics, Oxford University Press (2003).

- [18] M.A.H. Vozmediano, M.I. Katsnelson, and F. Guinea, Gauge fields in graphene, *Phys. Rep.* **496**, 109 (2010).
- [19] D. Sinha and B. Berche, Quantum oscillations and wave packet revival in conical graphene structure, arxiv/1509.00046.
- [20] E.R. Pereira, S. Fumeron, F. Moraes, Metric approach for sound propagation in nematic liquid crystals, *Phys. Rev. E* **87** (2013) 049904.
- [21] M.O. Katanaev and I.V. Volovich, *Ann. Phys.* **216**, 1 (1992); *Ibid.* **271**, 203 (1999).
- [22] P.S. Letelier, Spacetime defects: von Kármán vortex street like configuration, *Class. Quantum Grav.* **17**, 3639-3643 (2001).
- [23] B. Schutz, *A first course in general relativity*, Cambridge University Press (2009).
- [24] Y. Grats and A. Garcia, *Class. Quantum Grav.* **13**, 189 (1996).
- [25] O.D. Khvolson, *Grundzüge einer mathematischen Theorie der inneren Diffusion des Lichtes*, St Petersburg Academy Science **32** (1890).
- [26] A. Schuster, Radiation through a foggy atmosphere, *Astrophys. J.* **21**, 1-22 (1905).
- [27] K. Schwarzschild, Über das Gleichgewicht der Sonnenatmosphäre, English translation: Equilibrium of the sun's atmosphere, *Ges. Wiss. Gottingen Nachr. Math.-Phys. Klasse* **1**, 41-53 (1906).
- [28] M.F. Modest, *Radiative Transfer*, Mcgraw-Hill College (2003).
- [29] S. Chandrasekhar, *Radiative transfer*, Dover publications (1960).
- [30] L.A. Apresyan, Y.A. Kravtsov, *Radiation Transfer - Statistical and Wave Aspects*. Gordon and Breach Publishers (1996).
- [31] A. Maréchal, *Proc. Handbuch der Physik* **24** (3). Springer Verlag (1968).
- [32] C.W. Misner, K.S. Thorne, J.A. Wheeler, *Gravitation*. W H Freeman and Co (1973).
- [33] G.C. Pomraning, *The Equation of Radiation Hydrodynamics*. Pergamon, New York (1973).
- [34] S. Fumeron, F. Asllanaj, On the foundations of photon transport inside refractive media, *JSQRT* (2009).
- [35] M. Horz, P. Haupt, On the principle of Fermat in elastodynamics, *Continuum Mech. Thermodyn.* **7** (1995), 219-230.

